IN-18
050113

Submillimeter Wave Astronomy Satellite (SWAS) Launch and Early Orbit Support Experiences*

S. Kirschner, J. Sedlak, M. Challa, A. Nicholson, A. Calder, C. Sande, and D. Rohrbaugh†
Computer Sciences Corporation
Lanham-Seabrook, MD, USA 20706

Abstract

The Submillimeter Wave Astronomy Satellite (SWAS) was successfully launched on December 6, 1998 at 00:58 UTC. The two year mission is the fourth in the series of Small Explorer (SMEX) missions. SWAS is dedicated to the study of star formation and interstellar chemistry. SWAS was injected into a 635 km by 650 km orbit with an inclination of nearly 70 deg by an Orbital Sciences Corporation Pegasus XL launch vehicle.

The Flight Dynamics attitude and navigation teams supported all phases of the early mission. This support included orbit determination, attitude determination, real-time monitoring, and sensor calibration.

This paper reports the main results and lessons learned concerning navigation, support software, star tracker performance, magnetometer and gyroscope calibrations, and anomaly resolution. This includes information on spacecraft tip-off rates, first-day navigation problems, target acquisition anomalies, star tracker anomalies, and significant sensor improvements due to calibration efforts.

1. Introduction

The Submillimeter Wave Astronomy Satellite (SWAS) was successfully launched on December 6, 1998 (UTC). Orbital Sciences Corporation's enhanced Pegasus model XL, 3-stage, expendable launch vehicle launched SWAS into a near circular (635 km × 650 km) and high-inclination (69.96 deg) orbit. The Orbital Carrier Aircraft used to air-launch the Pegasus off the California coast is an L-1011 stationed at Vandenberg Air Force Base. Only ground sites are supporting SWAS.

The Flight Dynamics attitude and navigation teams successfully supported the launch. This support included orbit determination, attitude determination, real-time monitoring, and sensor calibration. This paper describes experiences during the launch and early mission phases. This first section gives a mission description of SWAS, a description of the spacecraft along with its attitude sensors and various attitude modes, and a tracking complement description. The next sections describe launch attempts, release and transition to a Sun-pointing attitude, software performance, and navigation results for the first day. Anomaly resolution, star tracker performance, and gyroscope and magnetometer calibrations are reviewed in the following sections. The paper concludes by describing some of the lessons learned from this launch. An overview of the mission and the Flight Dynamics support requirements can be found in Reference 1.

Mission Description

The Small Explorer (SMEX) was conceived as a low-cost program featuring a short turnaround time of typically 3 years from mission selection until launch readiness. However, because of problems with the Pegasus XL launch vehicle, SWAS launch was delayed from May 1995 to December 1998. SWAS is the fourth spacecraft to be launched in the SMEX series; the first three are the Solar, Anomalous and Magnetospheric Explorer (SAMPEX) launched in July 1992, the Fast Auroral Snapshot Explorer (FAST) launched in August 1996, and the Transition Region And Coronal Explorer (TRACE) launched in April 1998. The fifth in the series is the Wide-Field Infrared Explorer (WIRE), launched in March 1999.

---

* This work was supported by the National Aeronautics and Space Administration (NASA) / Goddard Space Flight Center (GSFC), Greenbelt, MD, Contract NAS 5-31000.

† Currently with AI Solutions, Inc.

SWAS is designed for a 3-year lifetime with a 2-year science goal. Scientists are using SWAS to study molecular cloud compositions in the galactic plane by examining submillimeter spectral lines that cannot be studied using ground-based facilities. The spectral lines of interest correspond to transitions between energy levels in several chemical species, in particular: water molecule ($H_2{}^{16}O$), isotopic water ($H_2{}^{18}O$), oxygen molecule (O_2), atomic carbon (C), and isotopic carbon monoxide (^{13}CO), all of which emit in the 0.5-0.6 mm wavelength band. The data provide a mini-survey of these clouds to be used for the development of maps. The chemistry data indicate the primary means of radiative energy release from the molecular clouds, information needed for models of their temperature and pressure. This is central to understanding the gravitational collapse of molecular clouds, leading to the formation of stars and stellar systems. Additional studies include mapping local interstellar clouds, high spatial resolution studies of selected clouds, a full survey of galactic plane clouds, and examination of selected extragalactic objects.

Spacecraft Description

SWAS is a three-axis stabilized spacecraft with no thrusters. The science instrument is a single telescope operating in the submillimeter wavelength range. Figure 1 shows the SWAS spacecraft. Its attitude sensors and actuators are as follows:

- One charge-coupled device star tracker (CCDST)
- One inertial reference unit (IRU) consisting of three two-axis gyroscopes
- One digital Sun sensor (DSS)
- Six coarse Sun sensors (CSSs)
- One three-axis magnetometer (TAM) and a redundant Y-axis magnetometer
- One four-axis reaction wheel assembly (RWA)
- One three-axis magnetic torquer assembly (MTA)
- One bright object sensor (BOS)

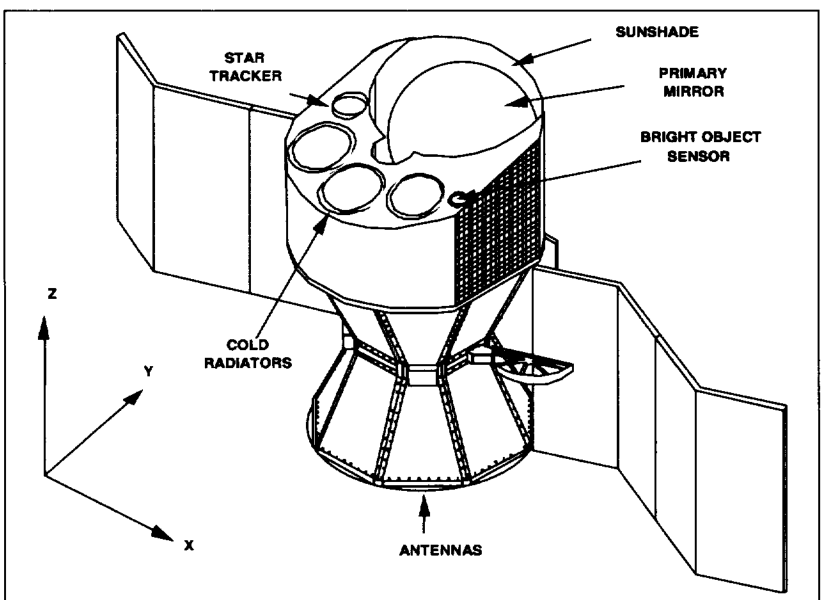

Figure 1. SWAS spacecraft.

The CCDST star tracker is the Ball Aerospace Systems Division model CT-601. It has an 8×8-deg field of view (FOV) and can track up to five stars at the same time. It is more sensitive to red stars than conventional fixed head star trackers, but this has been largely accounted for in the operational catalog of instrumental star magnitudes. The tracker is coaligned with the telescope boresight.

The IRU has three two-axis, tuned restraint inertial gyroscopes for redundancy. These gyroscopes are manufactured by Bell Textron and are of a type flown previously on sounding rockets. On some missions, the data adjustment for this type of IRU uses a different scale factor (counts to angle conversion) for rotations in the positive and negative sense. However, this asymmetry is currently thought negligible for the SWAS mission.

The BOS, a solar cell from Adcole, indicates whether the telescope pointing direction is satisfying Sun and Earth angle constraints. Other sensors and actuators share the SAMPEX heritage. Adcole manufactured the DSS and CSSs. The magnetometers and reaction wheels are from GSFC. Ithaco provided the MTA.

The SWAS personnel affiliated with Harvard's Smithsonian Astrophysical Observatory Science Operations Center (SAOSOC) in Cambridge, Massachusetts use the onboard-determined attitude for science data processing. Onboard attitude control algorithms use CCDST and IRU information with a minimum of uplinked commands (chiefly used to select targets). Because of the size of the star tracker's FOV and its ability to track multiple stars, the onboard closed-loop attitude control system (ACS) can determine accurate attitudes about the CCDST boresight (roll direction) using a single sensor. The required 3σ-control accuracy is shown in Table 1.

Table 1. SWAS attitude control accuracy requirements.

Rotation Axis	Science Control Mode		Non-Science Control Mode
	On-Target Pointing	Off-Target Pointing	
X and Y	± 57 arcsec (3σ)	± 90 arcsec (3σ)	Best Available*
Z (boresight)	± 38 arcmin (3σ)	± 38 arcmin (3σ)	Best Available*

*Dependent on control mode and available guide stars.

The control system also must keep the telescope boresight constrained to at least 75 deg from the Sun line and 35 deg from the Earth limb. Moreover, the fixed solar arrays — nominally normal to the spacecraft Y-axis — must point toward the Sun during orbit daylight to provide power. Y-axis deviations from the Sun line are restricted to rotations about the X- and Z-axes (telescope boresight) of ±15 and ±2 deg, respectively. SWAS has passive thermal control elements, but no thrusters and no known gas venting.

SWAS has five main ACS modes (listed in order of complexity):

1. Initial Sun Acquisition and Analog Safehold (momentum biased; analog control in hardware)
2. Digital Sun Point (DSP) (momentum biased; onboard computer control in software)
3. Inertial Sun Point (ISP) (boresight alternates pointing between North and South ecliptic poles; DSS and TAM data used for control)
4. Autonomous Stellar Acquisition (ASA) (boresight alternates pointing between North and South ecliptic poles; star tracker data used for control)
5. Stellar Pointing (SP) for normal operations

Ground commanding is needed to change from Analog Safehold mode to the others. The onboard system can autonomously order Analog Safehold or step down in the complexity of the control mode, as needed.

The ISP and ASA are safe "parking" modes. In these modes, the spacecraft alternates between North and South ecliptic poles, slewing roughly 180 deg about its Y-axis twice per orbit. During these rotations, the body Y-axis remains aligned with the Sun line. This keeps the spacecraft power-safe and the keeps the instrument FOV away from the Sun and Earth. If a target acquisition failure occurs while in SP, control reverts to ASA. If the spacecraft then cannot identify the pre-programmed star field near the ecliptic pole, it fails back to ISP mode where the attitude determination and control is based on the relatively coarse DSS and TAM data.

The Stellar Pointing mode can be further subdivided into Fixed Pointing, Nodding, and Mapping modes. In Nodding mode, the spacecraft remains inertially fixed as long as 45 seconds (sec) while on target, moves up to 3 deg off target (taking up to 15 sec for this motion), remains off-target for another 45 sec, and then moves back to the target. This process then repeats as often as needed for the observation. Mapping mode is similar, but the target is offset for each nod so that a map of the molecular cloud is built up over many nods. The spacecraft acquires three or four targets per orbit; hence *many* attitude maneuvers occur.

Tracking Complement Description

SWAS mission navigation is totally supported using range-rate tracking measurements. SWAS utilizes the Wallops constellation of Transportable Orbital Tracking System (TOTS) antennas currently located at Poker Flat, Alaska and Wallops Island, Virginia. These are 8-meter antennas that serve the SMEX series of missions using off-the-shelf components that have made the development and implementation of these antennas cheaper and quicker to implement than the larger standard antennas. During the first week following launch, the Deep Space Network's (DSN's) antennas located at Goldstone, Madrid, and Canberra augmented these antennas. In addition, due to the special consideration given to the paucity of early orbit tracking data, arrangements were made to obtain first-day tracking data from the Air Force C-band and North American Aerospace Defense Command (NORAD) B3 networks.

SWAS carries no thrusters, so no orbit maneuvers are possible after separation from the Pegasus XL launch vehicle. Table 2 presents the orbital requirements.

Table 2. SWAS orbital requirements.

	Position	Velocity
Predictive Ephemeris Accuracy After 14 Days	228 km (3σ)	60 m/sec (3σ)
OBC Along Track Knowledge Within 24-hr Span	50 km	60 m/sec

2. Prelaunch Activities and Early Results

The SWAS launch window for the planned launch on December 3, 1998 extended from 00:51 to 02:16 UTC. This window was selected to satisfy the constraint of keeping the spacecraft in full sunlight for at least the first five days. Launch was scheduled for 01:41 UTC near the end of the window to extend full sunlight by a day. The L-1011 took off at 00:43 UTC. Launch was aborted at 01:37 UTC and again at 01:53 UTC because the Western Range was not tracking the Pegasus. The L-1011 returned to Vandenberg Air Force Base at 02:30 UTC.

The second launch attempt was scheduled for 2 days later to allow for functional tests because the Pegasus XL had been airborne. The launch window was unchanged. Launch was planned for December 5, 1998 at 00:57 UTC, early in the window, because of predicted poor weather conditions. The launch attempt was aborted at 00:26 UTC with the L-1011 still on the ground because of the unfavorable weather conditions.

The schedule for the third launch attempt on December 6, 1998 was similar to the second. This time the launch was successful. The Pegasus was deployed from the L-1011 aircraft at 00:57:53.5 UTC, 59 minutes (min) after the L-1011 took off. SWAS separated from the Pegasus third stage at 01:09:34 UTC.

Post-Release Sun Acquisition

The initial position and velocity in geocentric inertial coordinates at the time of release from the Pegasus XL were (6435.824, -2479.835, 1292.382) km and (2.167318, 1.989943, -6.945519) km/sec, respectively. The first spacecraft telemetry was available as playback data only after the first orbit. Some of that initial telemetry for the attitude hardware is shown in Figure 2. The ACS was in Analog Safehold at release. The upper plot shows the Y-axis reaction wheel spinning up to its nominal safehold mode value of nearly 2300 revolutions per minute (rpm); the other three wheels remain commanded to zero. The spacecraft is momentum biased in this mode. The lower plot shows the Sun unit vector X- and Y-components in the SWAS body frame as measured by the DSS (the Z-component is similar to the X). The spacecraft settled into its nominal Sun pointing attitude for this mode after about 2500 sec with the Sun vector 16 deg from the spacecraft Y-axis.

Figure 3 shows components of the spacecraft angular velocity vector $\vec{\omega} \equiv (\omega_x, \omega_y, \omega_z)$. Since the gyroscopes were not powered on initially, the tip-off rates shown here could only be obtained indirectly. This was done by differentiating the spacecraft attitude history obtained from Sun and magnetic field measurements. By 2500 sec, Figure 3 shows SWAS has settled to its nominal coning motion with the transverse components ω_x (upper plot) and ω_z (not shown) exhibiting a sinusoidal behavior of amplitude 0.6 deg/sec and ω_y (lower plot) remaining constant at about 0.2 deg/sec. One feature of particular interest here is that the magnitude of the rate at release is approximately 1.5 deg/sec – well within the mission requirement of 4 deg/sec (Reference 2).

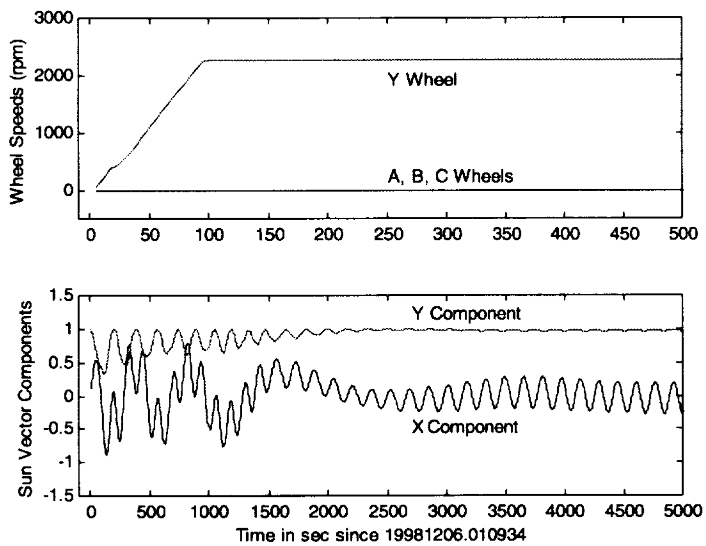

Figure 2. SWAS wheel speeds and digital Sun sensor unit vector X- and Y-components showing Sun acquisition in Analog Safehold mode just after separation.

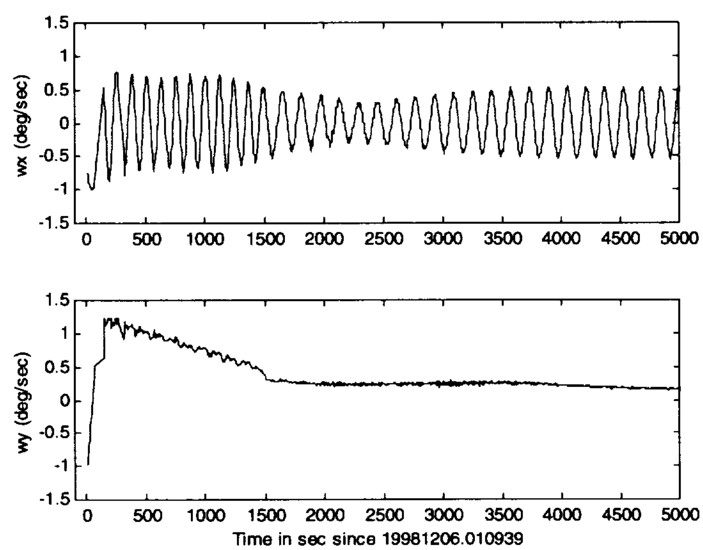

Figure 3. SWAS X-axis and Y-axis rotation rates after separation, obtained from derivative of single-frame attitude estimates.

3. Flight Dynamics Support Software

Navigation Software

The installation of navigation software in the SMEX Mission Operations Center (MOC) was intended to make the MOC a self-sufficient location in terms of providing navigation support. The suite of navigation software in the MOC is based around a core of Commercial-Off-The-Shelf (COTS) software from the Analytical Graphics Inc.'s Satellite ToolKit/Precision Orbit Determination System (STK/PODS) module, with modifications based on NASA defined formats added for end products to the tracking networks and other end users. This is the second mission supported using this technical approach (the first being TRACE and the third WIRE). The navigation software in the

MOC is a replacement for the legacy navigation software developed at GSFC and located in a second site at GSFC [the Multi-Mission Flight Dynamics facility's Mission Operations Room (MOR)].

The software in the MOC is limited in functionality during launch and real-time mission critical support. At the present time, it cannot ingest the NORAD and C-band data used in this launch. In its current configuration, the software is best suited for on-orbit operations, including orbit determination, orbital event planning, and scheduling products. During periods of rapidly changing solar activity, the software's usefulness is limited because the current configuration doesn't ingest the latest solar activity measurements. As a result, the legacy software is required during these periods to produce reliable orbit determination results. Consequently, at launch the legacy software processed the inertial guidance data and tracking data measurements from the Wallops networks, NORAD, DSN, and Air Force C-band stations. Then it provided orbital solutions and ephemerides for the MOC software to use in generating the planning and scheduling products. Improvements are planned to allow navigation support in the MOC to be independent of the legacy software in the MOR.

Attitude Software

SWAS is the first GSFC-supported mission for which all attitude support functions were carried out on PCs using the Windows NT operating system. The Attitude Determination System (ADS) was written in MATLAB. The major subsystems of the ADS are the Data Adjuster (DA), Star Identification function (STARID), Quaternion Estimator (QUEST), Batch-Least-Squares Estimator (BLS), Extended Kalman Filter (EKF), and Calibration functions (CAL). These and various other utilities were originally written for the Flight Dynamics Facility (FDF) Mainframe-to-Workstation transition, completed in 1997 (Reference 3 describes the original mainframe system). Thus these functions already have over a year of operational use in the FDF supporting six on-orbit missions. Porting the software from UNIX workstations to NT PCs required little effort since MATLAB works in both environments. Most of the ADS functions required little or no enhancement for SWAS mission requirements. The only new code development required for SWAS was a Telemetry Processor (TP), a driver and communication functions to enable real-time processing using the ADS subsystems, and two small functions for generation of calibration files for uplink to the spacecraft.

The Integration, Test, and Operations System (ITOS) unpacks the raw telemetry and produces text (non-binary) data files. The TP is a MATLAB function that reads the files, groups the data values by sensor/actuator, and passes the data on to the DA.

The Real-Time Attitude Determination System (RTADS) receives packets of data from ITOS via a TCP/IP socket. Low level functions to initialize and read data from the socket using the Winsock API were written in C. These low-level functions are called by a MATLAB real-time TP, which accumulates a user-specified number of data samples and returns to the RTADS main driver. The RTADS driver calls the DA, STARID, QUEST, and EKF functions, updates displays of results, and then calls the real-time TP for another cycle of data. Each cycle of adjusted data is concatenated to the previous cycle, so at the end of a real-time pass, the entire pass is in memory. This facilitates post-pass analysis of the real-time data. The performance of the RTADS was more than adequate to keep up with the telemetry data rate. No data was lost due to buffer overflow during any real-time pass.

The performance of the ADS in processing a 30 min span of typical playback data is summarized in Tables 3 and 4. The TP was the slowest subsystem due to the demands of reading, buffering, and parsing large volumes of text data; however, overall performance was adequate for mission support.

Table 3. Performance of Telemetry Processor.

Packet number	Data interval	Number of records	Processing time	Data contents
29	6 sec	300	3.9 sec	DSS, TAM, MTA, RWA, IRU (low data rate)
31	6 sec	300	2.2 sec	Star tracker (low data rate)
04	1 sec	1800	93.8 sec	OBC quaternion, star tracker, IRU (high data rate)

Table 4. Performance of Data Adjuster, Star Identification, and Batch-Least-Squares Estimator.

Subsystem	Processing time for 30 min of data
Data Adjuster	4.6 sec
Star Identification	5 sec
Batch-Least-Squares Estimator	5.9 sec

4. Navigation Results for First Day

The Pegasus final stage inserted SWAS into the final orbit on December 6, 1998 at 01:09:34 UTC. Table 5 compares the nominal orbital state, the orbital state reported via processing of the inertial guidance data, and the final orbit based on orbit determination results. The achieved orbit differed significantly from both the nominal orbit and the on-flight inertial guidance data estimate. These differences introduced relatively large positional errors for the supporting antennas during the first few hours of the mission. For previous Pegasus XL supports, the Orbital Sciences Corporation provided a post-injection assessment of the separation state using Global Positioning System (GPS) data to improve the positional estimate that has proven to be more reliable than the raw inertial guidance data. This vector was unavailable for SWAS.

Table 5. SWAS Separation and Post-Separation Vectors.

Parameter	Nominal Injection	Inertial Guidance Data – Post Injection	Orbit Determination Results
Epoch (UTC)	981206 010930.605	981206 010944.5	981206 010934.0
Semimajor Axis (km)	7045.7416	7024.8267	7028.6309
Eccentricity	0.004587	0.001279	0.001787
Inclination (deg)	69.9929	69.9593	69.9140
Right Ascension of Ascending Node (deg)	162.8101	162.8107	162.8387
Argument of Perigee (deg)	166.4561	152.2354	145.3064
Mean Anomaly (deg)	2.12077	17.0958	23.3095

Table 6 summarizes the tracking data used during the first day for SWAS. Poker Flat provided the only good tracking pass during the first few hours of the mission. Generally, orbit determination results for a new mission are not reliable for a ground-based tracking schema until the second pass. The second good pass did not occur until 8 hours after launch. By this time, the positional difference error for the supporting antennas had grown to nearly 100 km. Normal guidelines employed by navigation personnel are to try to keep positional differences under 35 km. Acquisition of the spacecraft was not interrupted due to this positional error.

Ultimately, the C-band and NORAD B3 tracking measurements were not useful during the first few hours of the SWAS mission to fill the holes in the DSN and Wallops network tracking coverage. To date, the passive tracking (C-band and NORAD) data types have proven not to be useful in the first few hours following Pegasus-based launches, perhaps due to the relative radar signatures of the Pegasus final stage and the spacecraft body itself. The TRACE and the Student Nitric Oxide Explorer (SNOE) spacecraft are other examples of this problem from 1998 launches. NORAD did correctly switch over the identification of SWAS to the proper object approximately 8 hours after launch. Caution should be given in the future for using these data types for Pegasus-based launches. However, these data types will continue to be sought for new missions until the era of GPS-based launch support is prevalent everywhere, especially for those missions where early orbit coverage by ground based antennas is spotty. These data types have been used with success for other launch vehicles and payloads, notably National Oceanic and Atmospheric Administration (NOAA)-K, which launched in May 1998. It should be noted that NORAD tracking data is generally delivered after a several hour delay to the MOR.

The early mission support for SWAS was further complicated by the need to assess whether an observation bias was needed in computation of the range-rate measurements from the TOTS antennas. Input to the TOTS receiver is down-converted, so subtracting 1980 MHz from the S-band downlink frequency determines the tuning frequency. The receiver can only be tuned in 100 kHz steps, which causes the range-rate data to have an observation bias. The range-rate bias is applied in the orbit determination measurement processing. The validation of whether to apply this bias is made on orbit to assess whether any other compensation for the bias has been made. For SWAS, it was determined that a 244.97 cm/sec bias must be applied using the Wallops WT3S data but no bias is needed using the Poker Flat WT1S data.

Table 6. SWAS tracking data for early orbit period on December 6, 1998.

Station (Antenna) & Location	Data Type	AOS HH:MM:SS	LOS HH:MM:SS	Data Quality	Maximum Elevation (deg)
WT1S Poker Flat AK	SRE USB30: Angles & Range-Rate	02:27:40	02:39:30	Good	21
KPTQ Kaena Point HI	C-band: Range & Angles	02:35:12	02:47:18	Bad (wrong object)	13
BELU	NORAD: Range & Angles	02:38:08	02:43:06	Bad (wrong object) & too low in elev.; data not received in real-time	4
KPTU Kaena Point HI	NORAD: Range & Angles	02:41:40	02:43:10	Bad (wrong object); data not received in real-time	13
CLAU Clear AK	NORAD: Range & Angles	04:12:17	04:12:40	Bad (wrong object) & too low in elev.; data not received in real-time	4
KPTQ Kaena Point HI	C-band: Range & Angles	04:13:18	04:28:48	Bad (wrong object); data not received in real-time	35
KPTU Kaena Point HI	NORAD: Range & Angles	04:21:30	04:23:00	Bad (wrong object); data not received in real-time	35
ASCU Ascension Island	NORAD: Range & Angles	05:12:12	05:15:21	Bad (wrong object) & too low in elev.; data not received in real-time	6
FY4U Fylingdales Eng.	NORAD: Range & Angles	05:28:37	05:33:57	Bad (wrong object) & too low in elev.; data not received in real-time	6
DS66 Madrid Spain	SRE USB85: Angles & Range-Rate	06:59:05	07:11:31	Bad (frequency shift mid-pass)	N/A
DS46 Canberra Aus.	SRE USB85: Angles & Range-Rate	07:47:37	07:57:04	Bad (ground station coherence problem until last few minutes of pass)	N/A
FY4U Fylingdales Eng.	NORAD: Range & Angles	08:52:03	08:55:43	Good; data not received in real-time	24
DS46 Canberra Aus.	SRE USB85: Angles & Range-Rate	09:28:10	09:37:10	Good	34
WT3S Wallops Island VA	SRE USB30: Angles & Range-Rate	10:13:20	10:23:40	Good	8
FY4U Fylingdales Eng.	NORAD: Range & Angles	10:27:00	10:35:50	Good; data not received in real-time	15
THUU Thule Greenland	NORAD: Range & Angles	10:27:24	10:33:47	Good but most data too low; data not received in real-time	6

Note: NORAD data was generally received several hours after the real-time event.

5. Anomaly Resolution

The SWAS mission proceeded smoothly during the first weeks after launch. Besides the expected minor troubles with data formats and the new software platform, there were some problems involving onboard systems and hardware that were potentially more serious. The spacecraft is designed to drop back to a lower control mode whenever it fails to acquire the targeted guide stars. When this occurs, the spacecraft leaves the planned timeline and opportunities for gathering science data may be lost, so resolution of control anomalies has a high priority. (The anomalies described here were solved by the joint efforts of Flight Dynamics personnel, the Flight Operations Team, the ACS engineers, and the visiting SAOSOC mission scientists working together as an extended team. The authors are not claiming or assigning credit for these efforts.)

One serious ACS problem was found when the spacecraft was commanded from ISP to ASA mode. These both are "parking" modes that are power safe and respect pointing constraints. In both modes, the spacecraft aligns the science instrument boresight near the North ecliptic pole for half of the orbit, then slews to the South ecliptic pole for the other half orbit. The two modes are distinguished by which sensors are used for onboard attitude determination. In ISP, the attitude is estimated using the Sun direction and the Earth's magnetic field vector. In ASA, the much more accurate star tracker data is used instead. When ASA mode was commanded, it was found that the star field could not be reliably identified after the 180 deg slew from one pole to the other, and the ACS would fail back to ISP mode. After reviewing plots of gyroscope and star tracker data from the playback telemetry, it was found that the spacecraft was acquiring its first guide star after the slew (the *base* star) before the motion had fully stopped. The star acquisition algorithm uses the base star to determine where in the FOV to look for the remaining four guide stars. If the spacecraft is still moving, it will not find them in the expected, small, directed search areas, and the star field acquisition will fail. The spacecraft motion in this case was due to a small attitude overshoot at the end of each slew. Once the problem was recognized, the ACS engineers were able to retune the onboard filter to remove most of the overshoot. This was accomplished by adjusting parameters involving deceleration of the rotation. This involved some trade-off with efficiency during other, smaller *nodding* maneuvers. These, in turn, were improved by adjusting the limits for switching between separate control laws for small and large maneuvers.

When the star tracker was powered on, there were cases where the electrical bus voltage limits were exceeded. This resulted in power to the star tracker being cut off, making fine pointing impossible. Hardware engineers verified with the star tracker manufacturer, Ball Aerospace, that voltages of that size also occurred on a similar test unit and were considered nominal when the tracker was used in that particular mode. The problem was resolved by changing the tolerances in the limit checks to be in line with actual behavior.

One extremely important science target that initially proved troublesome was the Orion Nebula. Star identification failed for this target repeatedly. When identification fails on a science target, the spacecraft falls back to ASA mode (that is, orientation toward the North/South ecliptic poles using star tracker control). However, before dropping back into ASA parking mode, the tracker performs a full field of view search. This yields the positions of the first five moderately bright stars. The onboard memory and computing power are not adequate to identify and use these stars, but they are crucial for ground analysis after the fact. We were able to identify these five stars using the pattern match algorithm in the STARID subsystem and readily verified that the spacecraft attitude was close to the commanded target. However, the star taken to be the base star by the onboard computer was identified by us to be the Orion Nebula itself. The combined magnitude of the bright Trapezium stars at the heart of the Nebula plus the integrated intensity of the Nebula itself add to an instrumental magnitude of 3.2, close to the expected base star magnitude. The base star is just over 0.5 deg from the Nebula while the onboard base star matching algorithm has a tolerance of 0.5 deg. The gyroscope misalignment, which had not been determined at that time, could easily have caused the Nebula to fall within the 0.5 deg window at the end of the slew to the Orion target. The simple solution was to choose an alternate base star farther from the Nebula. With this change, this target could be reliably identified. As is often the case, the solution is simple after the problem is correctly diagnosed.

Over the first few months of the mission, a number of isolated error events occurred where the CCDST briefly indicated saturation from a bright background and lost its lock on the guide stars. Fourteen events were identified and investigated through February 1, 1999. Of these, 12 were found to have occurred while SWAS was in the South Atlantic Anomaly (SAA) region. This is a region of relatively low geomagnetic field that allows a larger proton flux to impinge on the spacecraft. The other two of the 14 events occurred within 5000 km of either of the magnetic poles. The Sun, Moon, and Earth limb were checked for several of the events and could not be the source of the bright background, being too far from the CCDST boresight. The strong correlation with the SAA indicates that the isolated errors are very likely due to ionospheric charged particles interacting with the CCD or its electronics.

6. Star Tracker and SKYMAP Ground Star Catalog Performance

The performance of the SWAS CT-601 CCDST and the star identification results using the prelaunch SKYMAP ground star catalog allowed the determination of an accurate spacecraft attitude whenever the nominal complement of sensor data was available. The star identification algorithm is described in Reference 4.

The CCDST was commanded to track stars only during periods of inertial pointing due to the high slew rates required by the SWAS mission profile. During these times, the tracker reliably tracked commanded guide stars, only occasionally failing to acquire some guide stars. This failure occurred due to two distinct reasons. Early in the mission, the combination of the uncalibrated gyroscopes and attitude overshoot (even after retuning the control system) at the end of a slew could yield a large enough error to place a commanded star outside of the search field (see Section 5). This was a rare occurrence and did not degrade attitude determination since other commanded stars were successfully tracked. The other reason some fainter guide stars are missed is due to stray light interference from the bright Earth limb. This problem increased as the orbit precessed to a geometry where the Earth limb is necessarily nearer to the boresight for many important science targets.

New CCDST performance information was obtained during the SWAS science instrument calibration. This calibration involved exposing the telescope (and, hence, the coaligned CCDST) to a star field that included Jupiter (instrumental magnitude approximately −2.5). The CCDST tracked the commanded guide stars reliably despite the presence of a very bright planet in the sensor FOV.

The stellar magnitudes measured by the CCDST on SWAS were compared to magnitudes measured for the same stars by the two CT-601 trackers aboard the Rossi X-Ray Timing Explorer (RXTE) spacecraft. The predicted magnitude differences from the SWAS and RXTE SKYMAP ground star catalogs and the actual observed differences are shown in Figure 4. Differences are expected and arise from two main factors: the slightly differing shapes of the sensitivity curves for the CT-601 trackers involved, and the difference in the standard star chosen to establish a referent for the magnitude systems used for SWAS and RXTE (G0V standard star for SWAS; A0V for RXTE). The predicted differences from the ground star catalogs in Figure 4 agree well with the upper curve of Figure A-5 in Appendix A of the SWAS Run Catalog Prelaunch Analysis (Reference 5). As seen in Reference 5, the offset is due to the difference in referent stars while the slope is due to the difference in tracker sensitivity curves. The measured differences have a mean of 0.33 magnitudes, while the predicted differences have a mean of 0.46 magnitudes. The amount of SWAS data available is such that, given the inherent sensor noise, the measured differences cannot yet be separated into components reliably. A more detailed comparison should be possible in the future.

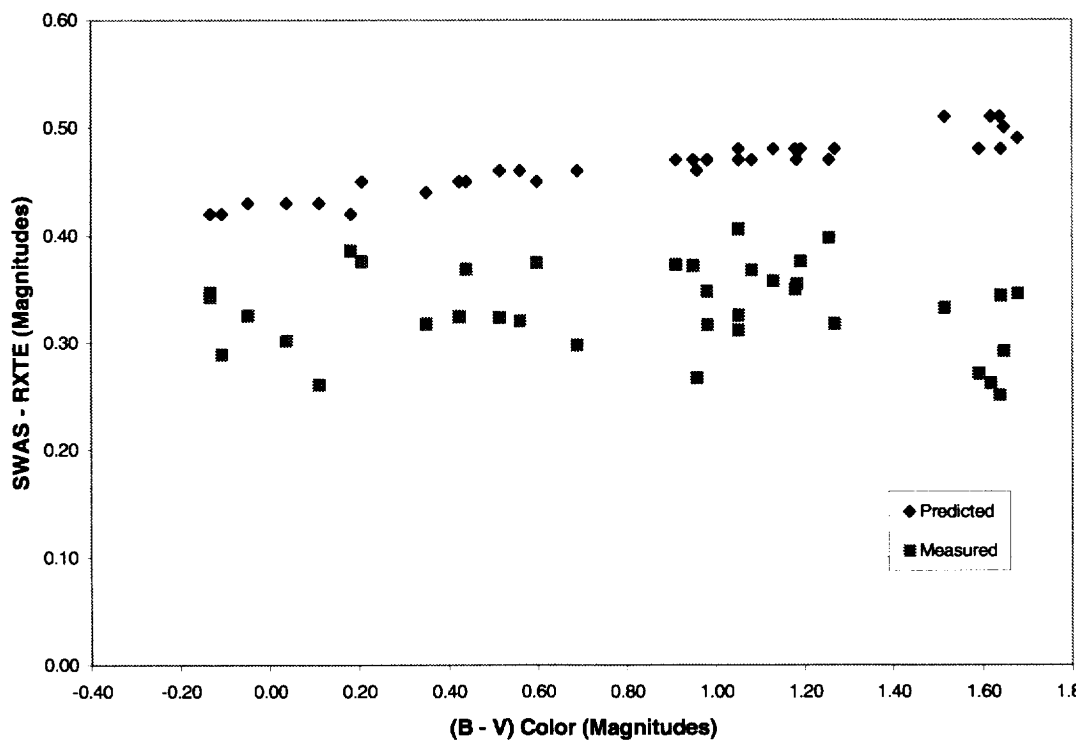

Figure 4. Predicted magnitude differences between SWAS and RXTE ground catalogs and measured differences for 37 stars observed by both spacecraft.

7. Calibration Results

Gyroscope Calibration

When the spacecraft performs a slew from one target to another, the final attitude must be close enough to the expected target to acquire the guide stars uplinked for that FOV. Once the star field is identified, the attitude is determined primarily from star tracker data. After that, the rotation rates from the gyroscopes are used in the on-board Kalman filter only to maintain a running weighted average of tracker data. However, during slews, the attitude is propagated purely on gyroscope data, so good calibration is crucial for consistent target acquisition. This is especially true for large angle attitude maneuvers.

As described in Section 1, the spacecraft reverts to ASA mode whenever it fails a science target acquisition. To ensure that ASA mode would work as a safe parking mode, it was planned to perform a partial gyroscope calibration during the first few days of the mission. The intention was to improve the accuracy of the twice per orbit North/South rotations to prevent dropping back to ISP mode. During these rotations, only the Y-axis of the gyroscope is exercised. The partial calibration uses attitudes and gyroscope biases estimated both before and after a Y-axis rotation. These attitudes are compared to the attitude determined from propagation using only the gyroscope rates. Any discrepancy is attributed to Y-axis gyroscope scale factor error. This neglects errors due to misalignment, which were expected to be smaller than the scale factor errors. (With only a single rotation axis, the available information is scalar, so only a single parameter can be estimated.) The first partial calibration was performed on December 7, 1998 while still in ISP mode. It was found that the prelaunch value of the Y-axis scale factor was low by 0.5% (a fractional correction of 0.005) which amounts to about 1 deg error for a 180 deg slew. However, these results were subject to significant uncertainty due to high sensitivity to the gyroscope bias determined using the Sun and magnetometer data before and after the slew. It was decided not to uplink a change to the scale factor until the partial calibration could be repeated using star tracker data from ASA mode. This was done on December 9, 1998 when a fractional scale factor correction of 0.0002 was found. This correction was small enough that no change to the onboard scale factor was considered necessary. It actually is consistent with zero scale factor correction, falling just within one standard deviation (1σ) uncertainty due to the errors inherent to the star tracker based attitude and gyroscope bias estimates.

A full gyroscope calibration (Reference 6) requires large rotations spanning all three axes. These could not be performed without violating Sun angle constraints while the spacecraft orbit was in full sunlight. It was planned to calibrate the gyroscopes three weeks after launch, giving time for the orbit to precess to a geometry where the shadow period was long enough to perform full 90 deg slews on all axes. In the interim, a full calibration using moderate sized slews was performed on December 20, 1998. The slew angles about the X-, Y-, and Z-axes were 43, 90, and 27.9 deg, respectively, with rotations in both the positive and negative sense. These 6 rotations plus an inertial hold of 23 min were used for the calibration. Gyroscope propagation errors for these 7 intervals were minimized over the set of 12 parameters including biases, scale factors, and misalignments for each axis. The results are given in Table 7, which shows the differences between the new calibrated values and the prelaunch values. The Y-axis fractional scale factor correction of −0.00015 is consistent with the partial calibration result of +0.0002, within the latter's uncertainty. The largest error is a rotation of 265 arcsec of the Y-axis. The X- and Y-axes both have a large component of rotation about the body Z-axis equal to −254 arcsec. Note that the X- and Y-axes are part of a single 2-axis gyroscope for this IRU configuration, so their common rotation angle indicates a simple misalignment of that gyroscope as installed in the body frame rather than any nonorthogonality in the gyroscope itself. These large X-axis and Y-axis misalignments lead to a propagation error of over 0.1 deg for a 90 deg Y-axis slew. An error of this size could explain why there was difficulty acquiring some science targets prior to the calibration. As mentioned in Section 5, the initial difficulties in acquiring the Orion Nebula guide stars probably trace to this misalignment.

Table 7. Differences between prelaunch and on-orbit gyroscope parameters based on calibrations performed on December 20, 1998 and January 13, 1999.

		X	Y	Z
December 20, 1998	Fractional scale factor correction	-0.00030	-0.00015	-0.00198
	Rotation of sensitive axis (arcsec)	256	265	115
January 13, 1999	Fractional scale factor correction	-0.00025	-0.00027	-0.00198
	Rotation of sensitive axis (arcsec)	242	255	121

The full calibration was repeated on January 13, 1999 using 90 deg slews about all three body axes. Table 7 shows both the December 20 and the January 13 calibrations for comparison. The scale factor corrections agree well within the uncertainties, and the alignments of the sensitive axes also agree closely. All the results are consistent within the error tolerances.

The calibration parameters were validated by comparing gyroscope propagation using rates adjusted with prelaunch and with on-orbit calibration values. The test is to propagate the attitude through slews distinct from the calibration slews and to demonstrate that the error angles are substantially smaller using the on-orbit calibration values. Table 8 shows the results using prelaunch values and Table 9 shows the results using the on-orbit calibration values from the full 90 deg slews. The propagation errors are much smaller using the on-orbit calibration. The average of the root-sum-squares (RSS) of the errors for the three axes is 498 arcsec for the prelaunch values and 44 arcsec for the on-orbit values, a factor of 11 improvement. Expressed as an accumulated error per degree of rotation, the prelaunch error was 5.5 arcsec/deg and the post-calibration error is 0.5 arcsec/deg, on average.

Table 8. Attitude propagation errors using prelaunch gyroscope calibration.

	X-error (arcsec)	Y-error (arcsec)	Z-error (arcsec)	RSS (arcsec)
+90 deg X-axis rotation	124.8	293.5	338.4	465.0
-90 deg X-axis rotation	101.6	216.5	156.2	285.7
+90 deg Y-axis rotation	116.4	202.8	368.0	436.0
-90 deg Y-axis rotation	353.6	53.0	129.2	380.2
+90 deg Z-axis rotation	212.1	123.9	696.4	738.5
-90 deg Z-axis rotation	18.9	85.5	676.4	682.0
Average propagation errors	154.6	162.5	394.1	497.9

Table 9. Attitude propagation errors using January 13, 1999 on-orbit gyroscope calibration.

	X-error (arcsec)	Y-error (arcsec)	Z-error (arcsec)	RSS (arcsec)
+90 deg X-axis rotation	41.7	28.9	11.4	52.0
-90 deg X-axis rotation	21.3	12.6	10.0	26.7
+90 deg Y-axis rotation	13.3	15.3	1.9	20.3
-90 deg Y-axis rotation	12.0	66.8	6.5	68.2
+90 deg Z-axis rotation	6.6	12.2	80.4	81.6
-90 deg Z-axis rotation	7.2	8.4	10.6	15.3
Average propagation errors	17.0	24.0	20.1	44.0

The most important test of the calibration is to verify that the spacecraft actually performs better using the new values. A measure of this is the size of the first onboard Kalman filter update of the attitude using star tracker data at the end of an attitude maneuver (the star tracker is not used during the slew). The tracker data is heavily weighted in the filter, so the change in the onboard estimated attitude in this first update step is close to the true propagation error. Averaging this measure of the propagation error from five slews before and five slews after uplinking the December 20, 1998 calibration parameters, it was found that the mean error angle was reduced by a factor of 6 from 378 arcsec to 64 arcsec.

Magnetometer Calibration

The TAM telemetry is processed onboard SWAS using the following model (Reference 7):

$$B_{adj} = R\, B_{counts} + b - C\, D$$

where:

B_{adj} = adjusted measured magnetic field vector in the spacecraft frame

R = *diagonal* matrix of scale factors

B_{counts} = vector of TAM measurements in counts

b = bias vector

C = torquer contamination matrix

D = vector of torquer dipole moments

The TAM residuals are then defined as $B_{adj} - B_{pred}$, where B_{pred} is the predicted field computed using the attitude estimate and the reference magnetic field in the inertial frame.

Note that the onboard TAM model does not include possible misalignments of the magnetometer axes with respect to the spacecraft body frame. Ground calibration of the 15 components of R, C, and b in this model was accomplished using an attitude-dependent calibration algorithm developed specifically for this TAM model (Reference 8).

On Day 2 of the mission, SWAS ACS engineers determined the contamination matrix, C, using an in-flight calibration algorithm that directly examines the effects of the magnetic torquers on the TAM measurements. However, these results showed that the prelaunch value of C was adequate and no changes were effected at that time.

Flight Dynamics personnel performed a preliminary TAM calibration using one orbit of DSP mode data from Day 2 of the mission, the main feature of interest being the significant and sustained torquer activity during this mode. A minor disadvantage of this procedure is that, during the DSP mode, the TAM itself (along with the DSS) generates the attitude data necessary for the calibration. The calibration was validated by carefully monitoring the TAM residuals over a two week span after the spacecraft entered the Stellar Pointing mode, since fine attitude profiles could be generated in this mode using only CCDST and gyroscope data. This validation indicated a need for a minor additional adjustment of the Z-axis bias by 2 milliGauss (mG).

Table 10 shows the effects of calibrating the TAM. This table presents the mean and root-mean-squares (RMS) residuals for components along the spacecraft X-, Y-, and Z-axes. It also shows the statistics of the field magnitude residuals, which are the differences between the magnitudes of the measured and predicted fields (indicated as "Mag" in the table). Note that, in Table 10, the mean residuals vanish for the DSP mode data set since this data set itself was used to estimate the TAM calibration parameters. Sample residuals are also shown graphically in Figure 5. It is clear from Table 10 that calibration significantly reduced the TAM residuals; for example, the RSS residual decreases from 9.6 mG to about 2.8 mG. Thus the TAM calibration was successful in that small magnetic field residuals were obtained consistently. It should be noted that the Flight Dynamics values for the contamination matrix differed from the prelaunch values by only about 2%; the major improvements in the residuals arose from estimating the X-axis and Z-axis biases, which were of the order of 10 mG.

Table 10. Statistics of SWAS TAM residuals before and after calibrating the TAM (upper number in each cell indicates mean residual; lower number indicates RMS residual).

Data Span	ACS Mode	Residuals before calibration: Mean (mG) RMS (mG)				Residuals after calibration: Mean (mG) RMS (mG)			
		X	Y	Z	Mag	X	Y	Z	Mag
6000 sec on Day 341 starting 1207.011432	DSP	2.76 5.68	2.44 2.83	3.49 6.47	-6.72 8.49	0.0 1.48	0.0 1.32	0.0 1.25	0.22 1.48
6000 sec on Day 342 starting 1208.000028	SP	3.27 4.90	2.38 2.43	6.39 9.16	-7.09 8.88	0.39 2.54	-0.09 0.58	0.17 2.17	0.50 1.51
10000 sec on Day 344 starting 1210.101007	SP	3.67 5.76	2.22 2.35	6.23 9.25	-9.00 10.13	-1.56 2.64	0.11 0.59	0.34 1.24	0.47 1.75
4000 sec on Day 351 starting 1217.003120	SP	0.63 4.19	3.03 3.15	3.96 6.45	-4.92 6.38	-0.61 1.77	0.40 0.71	-0.08 1.27	-0.68 0.98
6000 sec on Day 353 starting 1218.235902	SP	3.20 4.91	2.94 3.09	4.50 6.83	-5.48 7.04	-0.68 2.67	0.40 0.80	-0.57 1.26	0.51 1.69

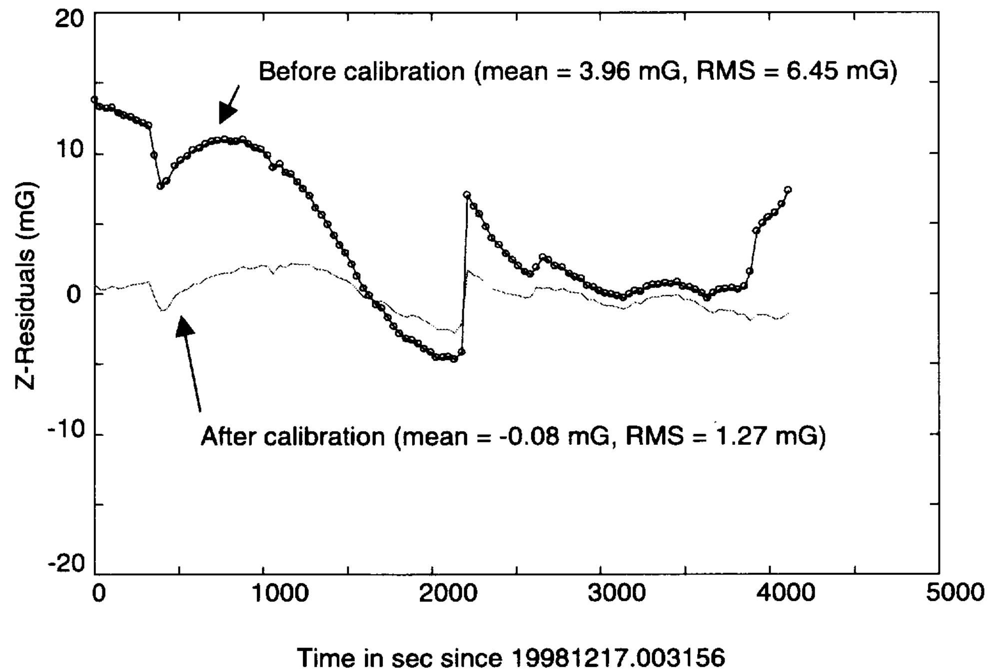

Figure 5. Typical TAM residuals showing the effects of calibration.

8. Conclusions

SWAS Flight Dynamics launch support succeeded by many different measures. The following highlights summarize the key experiences and lessons learned during early mission:

- The ground support software (also being used by the TRACE and WIRE missions) performed extremely well. Algorithms for identifying stars, determining attitude, and calibrating gyroscopes and magnetometers enabled the Flight Dynamics team to support the mission and help resolve anomalies.
- In order to improve chances of getting a stable orbit solution as soon as possible, there was the need for a variety of tracking sources during the first day of the mission. However, several bad early passes, slightly non-nominal injection, poor quality inertial guidance data, and early poor viewing geometry delayed attaining the first stable solution. Even with alternative tracking sources available, early tracking success may be limited for Pegasus-based missions.
- The SWAS star catalog, enhanced based on extensive RXTE star tracker analysis, helped improve the star identification process.
- Using attitude software that was developed in MATLAB allowed for easier modifications without disturbing configured software and the ability to perform quick analysis.
- Flight Dynamics personnel contributed to the analysis and resolution of the following spacecraft anomalies: attitude overshoot at the end of each slew; failure to target the Orion Nebula; and occurrence of CCDST single event upsets during SAA passage.
- Calibration of the gyroscopes reduced RSS average attitude residuals for a set of six 90-deg validation slews by a factor of 11. The gyroscope calibration allows the control system to maneuver more accurately to specified science targets, which, in turn, yields a higher acquisition rate of those targets.
- The magnetometer calibration reduced the TAM residuals from an RSS average of 9.6 mG to 2.8 mG. This is equivalent to improving coarse attitude solutions for contingency conditions by a factor of 3 or 4 yielding an accuracy of roughly 0.5 deg.

Many of these successes, particularly the resolution of anomalies, were greatly helped by the co-location of the Flight Dynamics launch support team with the Flight Operations Team and the ACS engineers. Co-location of personnel in the SMEX MOC was a great asset during resolution of the attitude overshoot problem, in particular. Communication among these groups was excellent and allowed for a rapid exchange of data and information regarding the anomalies as well as the analyses performed to interpret them. Solutions were formulated quickly and validated immediately after being uplinked to the spacecraft. This team effort resulted in the successful launch and early mission support of SWAS.

Acknowledgment

The authors would like to thank all of the SWAS Flight Dynamics team members for their many long and often late-night hours of effort that made this support a success.

References

1. S. Kirschner, *Submillimeter Wave Astronomy Satellite (SWAS) Flight Dynamics Support System (FDSS) Requirements Specifications, Revision 1*, Goddard Space Flight Center, 553-FDD-93/017R1UD0, April 1998

2. Orbital Sciences Corporation, *Pegasus (P20) SWAS Final Mission Analysis*, OSC Document No. TD-0619, Rev. A, November 4, 1998

3. J. Landis, et al., *Multimission Three-Axis Stabilized Spacecraft (MTASS) Flight Dynamics Support System Functional Specifications, Revision 1*, Goddard Space Flight Center, Flight Dynamics Division, 554-FDD-91/070R1UD0, September 1995

4. W. Daniel, T. Correll, and M. Anderson, "Development of a Direct Match Technique for Star Identification on the SWAS Mission," *Proceedings of the Flight Mechanics/Estimation Theory Symposium*, NASA Goddard Space Flight Center, May 1995

5. A. Miller, "SWAS Run Catalog Prelaunch Analysis," Computer Sciences Corporation, Memorandum 56830-04, September 9, 1996

6. J. Keat, *Gyro Calibration Analysis for the High Energy Astronomy Observatory-A (HEAO-A)*, Computer Sciences Corporation, CSC/TM-77/6082, June 1977

7. M. Anderson, *Small Explorer Program SWAS Attitude Control Software Algorithm Document, Build 3, Revision P*, NASA Goddard Space Flight Center, September 9, 1996

8. M. Challa, "Calibration Algorithms for Magnetometers Without Misalignments," Technical Memorandum No. CSC-86-910-20, Computer Sciences Corporation, September 1998